

# Thermal analysis for the high duty cycle PIMS accelerator

LIU Hua-Chang(刘华昌)<sup>1)</sup> PENG Jun(彭军) RUAN Yu-Fang(阮玉芳) FU Shi-Nian(傅世年)

Accelerator Center, Institute of High Energy Physics, CAS, Beijing 100049, China

**Abstract** To develop the high power proton linear accelerator for the Accelerator Driven System (ADS) program, the preliminary design of the Pi mode accelerating structure (PIMS) has been carried out. It is estimated that PIMS would heat up to 80 °C for low duty cycle (0.1%) without water-cooling, which is not acceptable, thus water-cooling is demanded. The structure stability for the high duty cycle or even for CW operation is crucially important for the ADS application. Therefore, thermal analysis with water-cooling for a high duty accelerator in our ADS research is performed to control the frequency shift caused by a temperature rise.

**Key words** PIMS, high duty cycle, thermal analysis, water-cooling

**PACS** 41.20.Cv, 44.05.+e, 44.10.+i

## 1 Introduction

High-power proton linacs have wide applications in neutron spallation sources, neutrino factories, transmutation of nuclear wastes and clean nuclear power production. These linacs are intended to deliver proton beams of up to several MW and operate with a continuous wave (CW) or pulsed high intensity beams [1]. The linac usually consists of different accelerating structures at the low- $\beta$ , medium- $\beta$  and high- $\beta$  sections. An elliptical superconducting cavity is generally chosen for the high- $\beta$  section. For the low and medium- $\beta$  sections, a room-temperature structure is commonly adopted, such as the radio-frequency quadrupole (RFQ) linac at low- $\beta$  section and the drift tube linac (DTL) or coupled-cavity drift tube linac (CCDTL), side coupled-cavity linac (CCL) and annular ring coupled structure (ACS) [2, 3] for the medium- $\beta$  section. Recently a new accelerating structure named Pi mode accelerating structure (PIMS) operating at room-temperature is proposed for the medium- $\beta$  section. Compared with the commonly used Pi/2 mode accelerating structure at room-temperature, PIMS has several advantages. First, PIMS can be used at the same frequency as the low- $\beta$  section accelerators, whereas the Pi/2 mode accelerating structures are often used at frequencies 2–

3 times that of low- $\beta$  section accelerators [4]. From the point of view of controlling the beam loss, it is better to have no frequency jump for a low-energy high-intensity beam with a strong space-charge effect. Secondly, for PIMS, the cells are coupled to adjacent cells through coupling slots on cell walls; a smaller number of cells are required for the same structure length. Thirdly, construction, tuning and operation of the PIMS are simpler.

In our ADS demonstration facility design, the linac consists of a 3.5 MeV RFQ, a 97 MeV DTL and a 167 MeV PIMS. The cavity design of the PIMS is started with the 2D code SUPERFISH [5]. The calculation to determine the coupling coefficients is made with a 3D electromagnetic field code. As the PIMS is designed to operate at a high duty cycle of 10%, the high heat load around the edges of the coupling slots and cavity noses becomes an important engineering constraint. Thus special care is required during the design of the cooling channels.

## 2 PIMS cavity design

The PIMS is composed of 14 cavities of 7 cells each, for a total of 98 cells covering a length of 25 m. The main design parameters are presented in Table 1, and

---

Received 1 September 2009

1) E-mail: liuhc@mail.ihep.ac.cn

©2010 Chinese Physical Society and the Institute of High Energy Physics of the Chinese Academy of Sciences and the Institute of Modern Physics of the Chinese Academy of Sciences and IOP Publishing Ltd

a 3D structure plot of a PIMS cavity is shown in Fig. 1. The cell length is the same within one and the same cavity, but changes from cavity to cavity according to the beam velocity profile.

Table 1. Main PIMS parameters.

frequency	352.2 MHz
energy range	97.05–167.5 MeV
electric gradient	3.8–4 MV/m
Max. surface field	1.8 Kilpatrick
beam current	40 mA
total power per cavity	0.9–1.1 MW
duty cycle	10%
beam aperture	4 cm
tank diameter	54 cm
wall thickness	2.5 cm
effective shunt impedance per length*	23.4–28.3 M $\Omega$ /m

\*SUPERFISH values for  $ZT^2$  were scaled by a factor of 0.7 due to additional losses.

The PIMS cell is optimized using the SUPERFISH code with the aim to maximize the shunt impedance and avoid voltage breakdown. The cell's diameter is adjusted to give the desired resonant frequency. The thickness of the walls between adjacent cells is determined by the power dissipation and cooling-channel requirements. A big beam aperture should be chosen because the focusing magnets are placed between the cavities, though a big aperture decreases the transit time factor. The cells are coupled by two coupling slots on the cell wall, which are turned by 90 degrees from cell to cell in order to minimize the second neighbor coupling. Generally, a large slot opening increases the coupling constant at the expense of lowering the shunt impedance [6]. After calculating various slot sizes with a 3D electromagnetic field code, we decided to use a 3.3% coupling factor, for which the effective shunt impedance  $ZT^2$  and the quality factor is reduced by about 10.7% and 15.3% respectively.

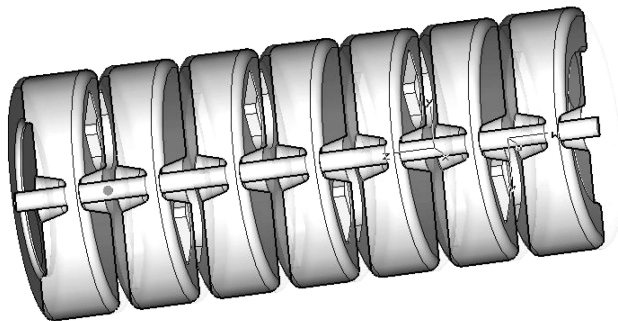


Fig. 1. Cross-section of a PIMS 7-cell cavity.

### 3 Heat flux

In addition to the electromagnetic design of the cavity shape, the cooling channel design is also very essential for a high-duty accelerating cavity, because the heat from RF power loss on the cavity wall will result in a cavity shape deformation and thus to a frequency instability during operation. To make a thermal analysis the heat flux loads are calculated with the ANSYS high frequency electromagnetic analysis module. The solid model of the PIMS is imported into ANSYS rather than being created internally. Actually, the solid model must include the cavity volume and the vacuum volume. Moreover, it is important that the vacuum volume shares its outer boundary with the inner boundary of the cavity; otherwise the meshes between the two volumes will not be associated.

Creating an acceptable mesh is an important process, since the surface heat flux is highly dependent on the mesh density at the vacuum boundary. It is advisable to create a fine mesh in critical areas such as the edges of the coupling slot, while retaining a larger mesh in the body in order to reduce usage memory and run time. For this reason, the 1/8 cavity model was adopted so as to achieve a high precision.

Since magnetic field intensity of each node can be provided by ANSYS directly (Fig. 2), the heat flux load is calculated in the format of power dissipation with:

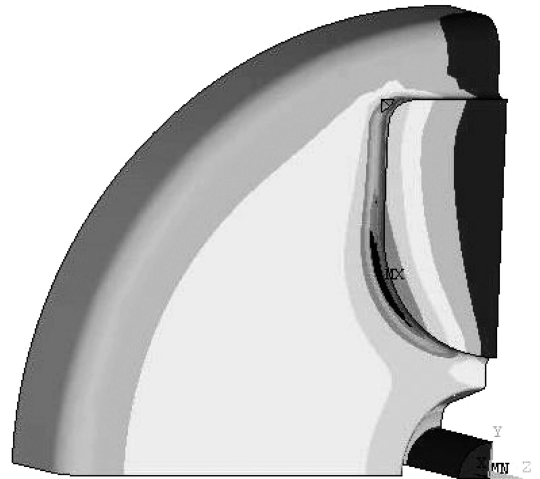


Fig. 2. Magnetic field ( $H$ ) distribution on 1/8 cavity model.

$$P = \frac{1}{2} H^2 R_f (\text{W/m}^2), \quad (1)$$

where  $R_f$  is the surface resistance of the material.

The calculated power loss is then normalized to the operation power of the cavity and used as a scaling factor for applying the heat flux load on the nodes.

#### 4 Temperature distribution water-cooling design

Once the heat flux loads have been applied and all electromagnetic quantities have been calculated, the electromagnetic mesh can be turned off. The cavity volume is now meshed with thermal elements, and the heat flux loads from the vacuum surface nodes is put on the cavity surface nodes. Fig. 3 is the temperature result, with the external convection in contact with air applied to the structure  $\left(h = 4 \frac{W}{m^2 K}\right)$  [7]. The following result is obtained for a heat flux corresponding to a 0.1% duty cycle.

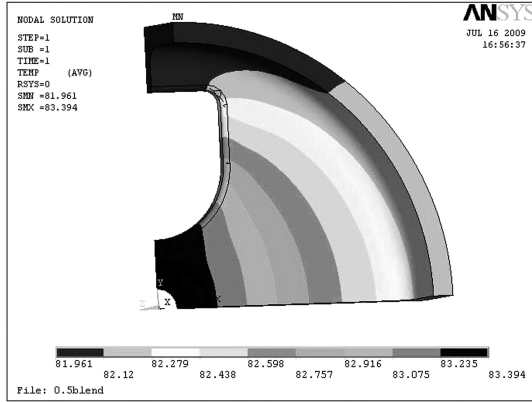


Fig. 3. Temperature distribution without cooling (0.1% duty cycle).

As can be seen from Fig. 3, the maximum temperature rises to 83.4 °C, which is consistent with our estimation. This situation is not acceptable. So we draw the conclusion that air convection alone cannot maintain the thermal balance, water-cooling channels must be added. Eight water-cooling channels including 2 inlets and 2 exits are arranged almost symmetrically on the cavity wall. The diameter of the water channel, mainly determined mechanically by the thickness of the cavity wall, is chosen to be 12 mm. Due to the high heat load around the edges of the coupling slots, additional channels are introduced to avoid any serious deformation of the coupling slot shape, as shown in Fig. 4. The distance between the cooling channel and the accelerating tube is 5 mm, and to keep the coupling slot away from deformation caused by water pressure, 8 mm distance between channel and slot is chosen.

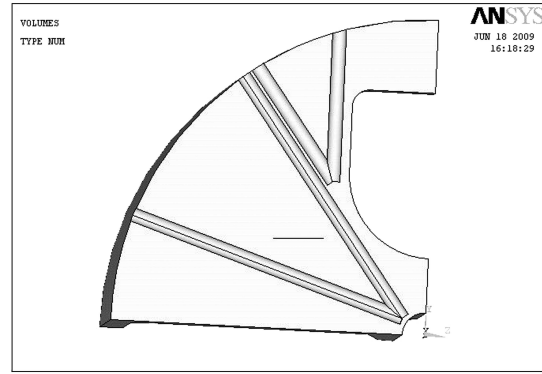


Fig. 4. Water-cooling channels layout.

#### 5 Thermal and structural analysis

To calculate the heat transfer coefficient  $h$  between the cooling water and the water-cooling channel surface one can use the Dittus-Boelter equation:

$$h = \frac{Nuk}{D}, \quad (2)$$

with

$$Nu = 0.023 \cdot Re^{0.8} \cdot P_r^{0.4} \quad (3)$$

$$Re = \frac{v \cdot D \cdot \rho}{\mu}, \quad (4)$$

here  $v$  is the velocity of the water flow,  $\mu$  is the absolute viscosity of water,  $\rho$  is the water density.  $P_r$  is the Prandtl number defined as [8]:

$$P_r = \frac{C_p \cdot \mu}{k}. \quad (5)$$

With a cooling water velocity of 2 m/s in the inlet pipe, the mass flow rate  $m=0.23$  kg/s, the specific heat capacity of water  $C_p=4200$  J/kg. The expected heat load per cell at 10% duty cycle is 9.5 kW, and the water temperature rise across the cavity is:

$$\Delta T = \frac{Q}{mC_p} = 5 \text{ } ^\circ\text{C}. \quad (6)$$

The simulation shows a maximum temperature of 43 °C at the nose tip. The temperature rise near the coupling slot seems a little bit smaller than the maximum one near the tip due to the effect of the additional cooling channel (Fig. 5).

To judge whether the frequency shift caused by RF power dissipation is out of control, a structural analysis has also been carried out. After thermal analysis, ANSYS allows the thermal elements to be converted directly to the structural elements in order to obtain the stress and displacement solutions. The

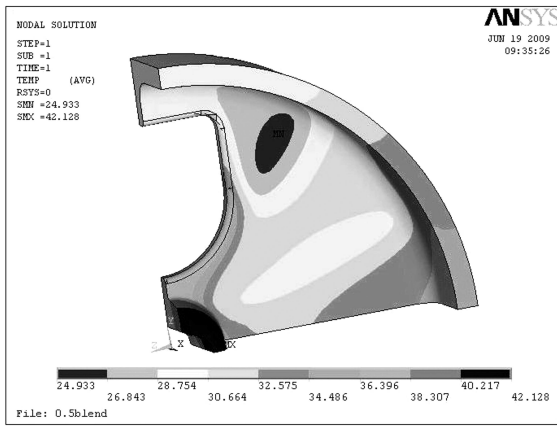


Fig. 5. Temperature rise with constant average cooling water temperature of 21 deg, and 10% duty cycle.

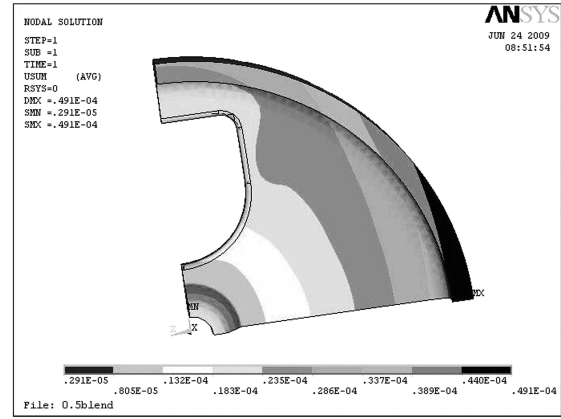


Fig. 6. Structural distortion.

thermal distortion of the cavity is based on the coefficients of the cavity materials and the nodal temperature data obtained from the thermal solution, which are applied as a load on the structural model. Based on the above results of thermal analysis, the calculated maximum deformation of the PIMS cavity is 49.1  $\mu\text{m}$ , as shown in Fig. 6. The nodal displacements at the cavity-to-vacuum interface are automatically added to the original nodal locations by using the UPGEOM command and a new RF model based on this profile is obtained to determine the frequency shift caused by the structural distortion. The structural distortion due to RF power dissipation results in a  $-123$  kHz frequency shift for the cavity, and the calculated frequency shift sensitivity to the temperature is about  $-10.5$  kHz/ $^{\circ}\text{C}$ . It is within control range.

## 6 Conclusions

In the above calculation the basic design of PIMS accelerating cavity has been accomplished. In order to remove the heat generated by the RF power dissipated on the inside surface of the cavity to maintain thermal stability and to limit the undesired deformation, properly water-cooling channels have been designed. According to the RF-thermal-structural simulation, the existing water-cooling design can satisfy the high duty cycle (10%) operation requirement and makes the PIMS accelerator work steadily at a proper temperature.

*The author would like to thank Prof. Ouyang Hua-fu and Dr. Xiao Yong-chuan for their valuable suggestions and discussions.*

## References

- Mosnier A et al. Survey of High-Power Proton Linacs. Proc. of Linac2002, 2002. 821–825
- Kustom R L et al. An Overview of the Spallation Neutron Source Project. Proc. of Linac2000, 2000. 321–325
- Accelerator Group. JAERI/KEK Joint Project Team. Accelerator Technical Design Report for J-PARC. JAERI, KEK, 2003
- Wegner R, Gerigk F. PIMS—A Simple and Robust Accelerating Structure for High Intensity Proton Linacs. NIMA, 2009, **606**(3): 257–270
- Billen J H, Young L M. POISSON SUPERFISH. LA-UR-96-1834, LANL
- Wangler T P. Principles of RF Linear Accelerators. New York: John Wiley & Sons, INC, 1998. 122
- Bourquin P et al. Development Status of the Pi-mode Accelerating Structure (PIMS) for LINAC4. Proc. of Linac2008, 2008. 939–941
- LIU Hua-Chang, OUYANG Hua-Fu. Chinese Physics C, 2008, **32**(4): 280–284